Metrol. Meas. Syst., Vol. 29 (2022) No. 1, pp. 37–51
DOI: 10.24425/mms.2022.138547

PAN POLSKA AKADEMIA NAUK

METROLOGY AND MEASUREMENT SYSTEMS
Index 330930, ISSN 0860-8229
www.metrology.wat.edu.pl

M&MS

COMPARATIVE ACCURACY ANALYSIS OF TRIANGULATED SURFACE MODELS OF A FOSSIL SKULL DIGITIZED WITH VARIOUS OPTIC DEVICES

Yaroslav Garashchenko[1)], Ilja Kogan[2,3)], Mirosław Rucki[4)]

1) *National Technical University, Kharkiv Polytechnic Institute, Department of Integrated Technologies of Mechanical Engineering, Kyrpychova Str. 2, Kharkiv, 61002, Ukraine* (*yaroslav.garashchenko@khpi.edu.ua*)
2) *TU Bergakademie Freiberg, Geological Institute, Bernhard-von-Cotta-Str. 2, 09599 Freiberg, Germany* (*ilja.kogan@geo.tu-freiberg.de*)
3) *Kazan Federal University, Institute of Geology and Petroleum Technologies, Kremlyovskaya Str. 4/5, 420008 Kazan, Russia*
4) *Faculty of Mechanical Engineering, Kazimierz Pulaski University of Technology and Humanities in Radom, ul. Stasieckiego 54, 26-600 Radom, Poland* (✉ *m.rucki@uthrad.pl*, +48 48 361 7697)

Abstract

Digital metrology was applied to evaluate 3D models of the unique skull of a fossil tetrapod, *Madygenerpeton pustulatum*, generated using various 3D digitization methods. The skull surface is covered by minute tubercles making it challenging for digitization with appropriate accuracy. Uniqueness and fragility of the specimen preclude the use of tactile measuring systems for creating a standardized reference model. To overcome this problem, comparative analysis of the triangulated models generated from the clouds of points obtained with seven different devices was conducted using the Geomagic Studio and Autodesk PowerShape CAD software. In the proposed approach, geometrically and dimensionally closest-fitting models underwent detailed statistical analysis between surface polygons in three steps. First, 3D models obtained from different scanning methods were compared with each other in couples. Next, statistical analysis of the differences between the coupled models was performed. Finally, a rating list of the models related to the required accuracy was prepared. The proposed approach is applicable to any other scanned object, especially in palaeontological applications, where each object is unique and exhibits individual features.

Keywords: Madygenerpeton, optical measurement, triangulated model, polygonal analysis, accuracy.

1. Introduction

Fossil remains of ancient organisms are unique documents of life in the geological past. Their individual appearance is determined by biological characteristics but also by the geological processes related to fossilization, resulting in different preservation patterns. Fossils are often fragile and can be easily damaged during transportation or plastic reproduction.

Article history: received June 23, 2021; revised September 30, 2021; accepted October 18, 2021; available online November 10, 2021.

Non-destructive or even non-contact digital methods offer various advantages for providing access to fossils for several groups of users (researchers, students, museum visitors, broader public). Digital models can be simultaneously viewed, manipulated on screen, or used for obtaining analogue (printed) copies without touching the actual object.

Several approaches to digital 3D imaging of macroscopic objects, generally based on light optics, laser optics or X-ray transmission are available. The most accessible method is photogrammetry which delivers a photorealistic 3D image but can encounter limitations with respect to relief features. Structured-light 3D scanners ensure sufficient resolution and dimensional accuracy with accompanying information on the surface texture. Laser-based scanners are able to scan surface geometries with very high resolution and usually smaller error. They exhibit negligible sensitivity to the daylight influence [1].

In reverse engineering, the applied software is crucial to producing a high-quality object reconstruction as well as for comparative analysis of the obtained 3D models. Among published papers, there is a report on the evaluation of 13 programs through the comparison of scanned models of four articulated human pelves [2]. Several methods of data collection were considered, such as structured light scanners, photogrammetry, and computed tomography. However, despite relatively long period of the development of scanning methods designed for reproduction and reverse engineering purposes, there are still important limitations in obtaining 3D models of an object without defects [1] and with the required high accuracy [3]. Among other factors, the accuracy of a 3D model can be seriously affected by improperly chosen scanning parameters or by insufficient qualification of the operator who prepares the object and performs the scanning procedure [4].

3D scanning is widely applied in various scientific disciplines, such as analysis of large engineering constructions [5], archaeology (*e.g.*, [6–12]), palaeontology (*e.g.*, [13–16]), anthropology (*e.g.*, [17]), and zoology (*e.g.*, [18–22]). An exhaustive review of the application of 3D scanning in medicine can be found in [23]. There are reports also on the application of 3D scanning in the analysis of historical paintings in order to evaluate 3D textural effects on the surface that create additional reflections for highlights or emphasise the textural appearance of the material they depicted [24]. The authors found it necessary to compare the feasibility of three 3D scanning techniques which have been used to capture the surface topology of the analysed painting. Sousa *et al.* [25] focused on the capability of several scanning methods to reconstruct a human head but the authors did not manage to point out any statistically sufficient differences in individual dimensions important from the anthropometric perspective. In engineering applications, assessment of scanning methods can be performed through comparison of certain surface parameters [26] or using an appropriate reference surface [27].

Numerous studies have been performed on 3D scanning in the area of stomatology [28–31]. The question of the proper scanning method able to model such complex objects as teeth in a human mouth was addressed in terms of dimensional accuracy [32]. The authors repeated scanning 20 times with each analysed method, automatically comparing twelve linear measurements on the digitized models using special software. For measurement accuracy analysis, they used one-sample t-test and one-way analysis of variance. Other authors [33] only reported high accuracy of the obtained models with insufficient differences of the critical dimensions in a similar study case.

Despite the number of papers dealing mainly with the feasibility of 3D scanning in various fields of science, there is no standard solution how to determine feasibility for any given application. The issue raises on the proper choice of a scanning method because of different sensitivity to the properties of the scanned surface, such as reflectivity, roughness, texture, geometrical features of small elements, *etc*. In addition, appropriate methods for quantitative evaluation of different digitization approaches of natural objects still have to be developed. While digital representa-

Metrol. Meas. Syst., Vol. 29 (2022), No. 1, pp. 37–51
DOI: 10.24425/mms.2022.138547

tion of specimens increasingly becomes standard in palaeontology [34], only one quantitative study evaluating 3D models of fossils obtained with different techniques has been published so far [35]. We are attempting to fill in this gap by comparing 3D surface models of the holotype of *Madygenerpeton pustulatum*, a fossil skull of highly complex surface geometry whose accurate representation in both digital (3D-scanned) and analogue (3D-printed) is challenging. Preliminary qualitative and semi-quantitative results and an evaluation of printed copies are presented in [36]. The present contribution was, after initial discussion [37], expanded with new results and calculations, new graphs, plots and final rating. It introduces the use of digital metrology for evaluating 3D models of a fossil and proposes a method for further objective evaluations in terms of required reproduction accuracy. Results of the evaluation can be used to substantiate the choice of the appropriate 3D digitization technology. Since metrological evaluations of the available devices based on standardized artificial objects do not shed any light on their ability to capture natural objects such as fossils, our approach is based on comparative statistical analysis of the 3D surface models generated with different scanning methods of known metrological characteristics. We believe that this approach is applicable to any other scanned object, and can be recommended for validation of scanning methods in each particular case when no reference model is available.

2. Materials and methods

Among the materials and methods, three main groups should be mentioned, namely, the measured object, the digitization devices, and the general approach to the analysis.

2.1. Measured fossil skull

We digitized the type specimen of the 'reptiliomorph amphibian' *Madygenerpeton pustulatum* [37] from the Triassic Madygen Formation of Kyrgyzstan. The holotype is a detached and slightly deformed skull lacking the lower jaw. Together with a few series of dorsal plates belonging to at least three individuals, the skull represents the only fossil evidence of this animal which looked and lived similar to a crocodile but was related closer to frogs. Besides a palaeontological interest in the *Madygenerpeton* skull for exhibitions, teaching, and research purposes, its challenging morphology characterized by numerous minute tubercles covering the surface of the bone makes it an object valuable for digital reproduction. The object is shown in Fig. 1. Magnified pictures of the *Madygenerpeton* bone surface were obtained using a KEYENCE VHX-5000 digital microscope in 3D mode and tubercles were measured with the digital measuring tools available.

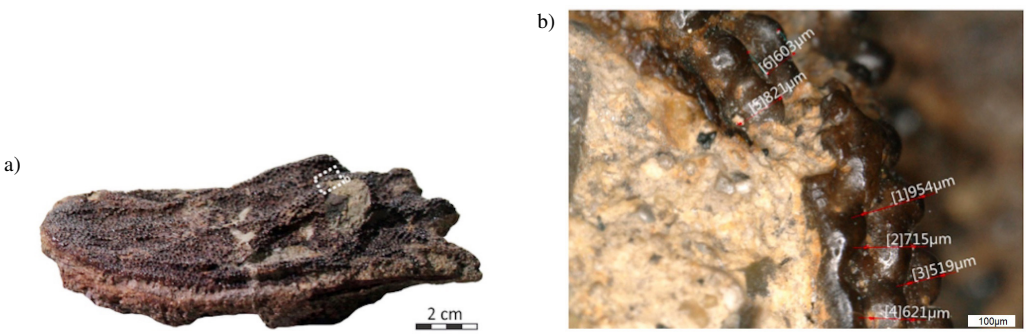

Fig. 1. Skull of *Madygenerpeton pustulatum* (holotype FG 596/V/4, TU Bergakademie Freiberg): a) general view and b) close-up picture of bony tubercles covering the skull in the region of left orbit [37].

2.2. Measurement systems

The following measurement systems were used in the experimental research, covering photogrammetry, structured light scanning, laser scanning, and coordinate measuring machines with laser probes. The scanning procedures were performed in laboratory conditions by professional operators.

Photogrammetry: some 300 pictures were taken with a Fujifilm X-T2 full-format system camera with a Fujinon Super EBC XF 10–24 mm 1:4 R OIS lens mounted on a tripod moved around an illuminated table on which the object was resting. A 3D model was computed using the 3DF Zephyr commercial software package. The software processes a point cloud from the pictures (we have obtained around 11.5 million points) and generates the final photo-realistic textured mesh via surface triangulation.

Handheld structured light scanning: the object was scanned on various occasions in different institutions with an Artec Space Spider, an EinScan Pro and a CREAFORM GoScan 3D. 3D models were generated in the respective scanner software.

Industrial structured light scanning: the skull was scanned with an AICON SmartScan at the State Archeological Survey of Saxony, Dresden. A 3D model was produced with specially developed software.

Laser scanning: the fossil was scanned with the handheld laser scanner CREAFORM HandySCAN 3D. A 3D model was obtained using CREAFORM software.

Coordinate Measuring Machines: The skull was measured at Mitutoyo Polska, Wrocław with the CMMs CRYSTA-Apex S 9166 and STRATO-Apex 574. The CRYSTA-Apex S had a measuring range of 900 × 1600 × 600 mm and a maximum permissible error $MPE_E = \pm(1.7+3L/1000)$ µm. The SurfaceMeasure 606 non-contact line laser probe was applied for surface scanning. Its scanning error was 12 µm [1σ/sphere fit]. The CMM STRATO-Apex had a measuring range of $500\times700\times400$ mm, a maximum permissible error MPEE = $0.7+2.5L/1000$ µm and 5 µm scanning error for roundness. It was equipped with a SurfaceMeasure 201FS non-contact line laser probe with a 1.8 µm scanning error.

Main technical data of the obtained models are collected in the Table 1.

Table 1. Characteristics of the obtained 3D models.

Characteristics	3D scanning devices						
	AICON	AR Crysta	ARStrato	ARTEC	Creaform GoScan	Creaform HandyScan	EinScan Pro
Device accuracy (from specification)	20 µm (Length measuring error)	$1.7+3L$ / 1000 µm (MPE_E)	$0.7+2.5L$ / 1000 µm (MPE_E)	50 µm (accuracy of 3D point)	$0.05+L$ / 6600 mm (MPE_E)	$0.02+L$ / 16,600 mm (MPE_E)	0.05 mm (automatic and manual mode)
Model type	Full model	Upper surface	Upper surface	Full model	Full model	Full model	Full model
Dimensions along the axes X, Y and Z, mm	109.159 31.605 68.883	108.797 26.058 66.757	106.289 20.132 65.100	110.546 31.674 69.062	108.846 31.314 68.687	108.846 31.352 68.720	109.085 31.371 68.841
Number of polygons (triangles), pcs	13,913,354	183,100	230,378	5,682,554	116,932	116,898	12,515,900
Surface area, mm^2	19,307.587	8,703.181	8,180.969	21,578.959	16,837.545	16,837.940	17,951.267
Model volume, mm^3	30,571.640	–	–	31,325.110	31,941.370	31,941.728	30,937.090

Metrol. Meas. Syst., Vol. 29 (2022), No. 1, pp. 37–51
DOI: 10.24425/mms.2022.138547

Unfortunately, accuracy was defined in specifications of different devices in different ways, because the choice of the scanning method involved many other criteria described in [36], apart from measurement accuracy.

2.3. Methodology of the analysis

In the accuracy analysis, CAD software packages Geomagic Studio and Autodesk PowerShape were used. These programs provide appropriate tools for comparison of 3D polygonal models and statistical analysis of the differences between the tested model and the reference one. Due to the uniqueness of the analysed object, no reference model was available for accuracy analysis. Thus, each couple of models underwent a comparison between each other. Comparative analysis was performed in two stages. First, coupled 3D models underwent visual and statistical analysis of the differences between them. Next, the models fitting closest, both geometrically and dimensionally, were chosen and underwent detailed statistical analysis of the differences between surface polygons (triangles). The results of the analysis provided a ground for accuracy rating as well as choosing one of the models as the reference one.

3. Results and discussion

The results are presented in three groups: coupling of the obtained 3D models from different scanning methods, statistical analysis of the differences between the coupled models, and rating of the devices with respect to the accuracy of the model.

3.1. Coupling of the models

Assessment of the scanned models allowed for the exclusion of the photogrammetry method from the further analysis. The photogrammetric model was initially adjusted manually to the AICON model and then it was scaled along X, Y, and Z coordinate axes according to the AICON model dimensions (109.159 × 31.605 × 68.883 mm). The initial dimensions of the photogrammetric model were 135.908 × 35.317 × 93.314 mm, so that the scaling was disproportionate along the respective axes X – 0.80318, Y – 0.89489, and Z – 0.73818. Analysis of the distances between two models, AICON and photogrammetry, indicated insufficient surface data for the analysis, as can be seen in Fig. 2.

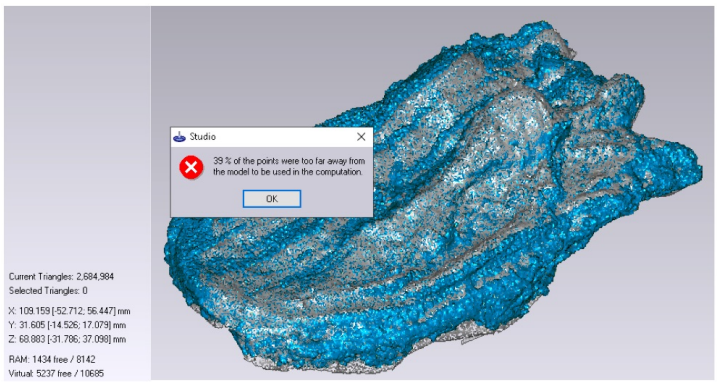

Fig. 2. Message on insufficient data for surface analysis of the photogrammetric 3D model.

The eventual result of the Photogrammetry-AICON comparative analysis showed the largest deviations. Average differences in outer and inner directions from the 3D AICON model were 0.361 mm and –0.794 mm, as it is presented graphically in Fig. 3. The overall square root of these deviations was 0.873 mm, which is larger than the dimensions of most of the bony tubercles that had to be represented.

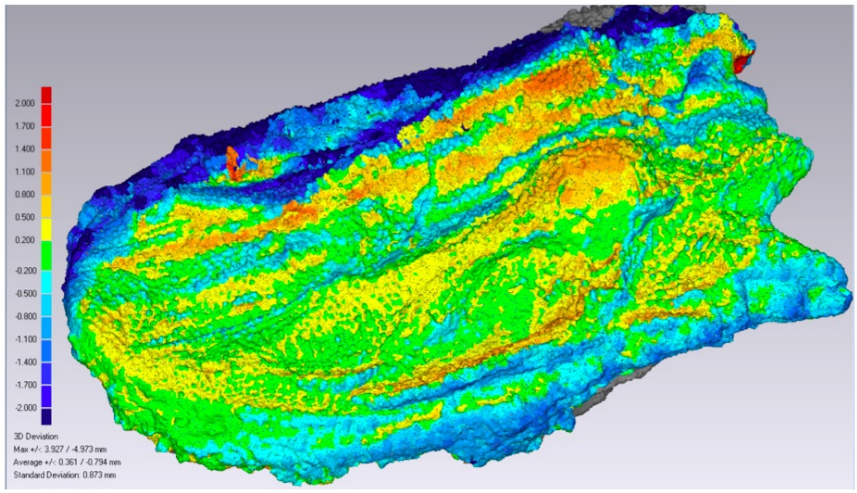

Fig. 3. Colour mapping of deviations between the photogrammetry and theAICON models.

It should be noted that there are reports indicating the issue with photogrammetry. For instance, Waltenberger *et al.* tested 13 different photogrammetric software tools comparing surface models and found out that "only one photogrammetric software package yielded surface models of the complete pelves that could be used for further analysis" [2]. The authors pointed out that "most photogrammetric methods capture only shape information" and dimensional fidelity requires manual calibration based on the scale. In the case of our fossil skull, while trying various scale coefficients in each dimension, it was possible to reduce the deviations. However, these results are essentially incorrect because of disproportional scaling of the object without clearly defined geometry, so that overall dimensions could not be determined accurately. Nevertheless, this model can be used to supplement other 3D representations since it allows to keep true colours and to obtain texture superposition.

Compared to 3D models obtained by structured-light scanning, the photogrammetric model of the *Madygenerpeton* skull is clearly inferior in terms of surface geometry reproduction. A reason might be that among the compared digitization techniques, the photogrammetric method is perhaps the one with the most potential uncertainties due to external factors. These include the operator's experience as well as the choice and the use of hard- and software. For instance, dimensional inaccuracy might have been caused by camera limitations or wrong photography settings, including sensitivity, aperture and exposure time, camera placement, *etc.*; by incorrect illumination; or, crucially, by the software applied for photogrammetric reconstruction. There are little comparative data on applying 3DF Zephyr for photogrammetry of fossils, and only some information is available on the more widely used software packages [35, 39]. For a more in-depth evaluation of the photogrammetric method in comparison with the other devices, further studies on this specimen using different photographic equipment and photogrammetric software must be performed.

Metrol. Meas. Syst., Vol. 29 (2022), No. 1, pp. 37–51
DOI: 10.24425/mms.2022.138547

Thus, it can be concluded that the data obtained from photogrammetry as it had been done by Kogan *et al.* [36] should not be recommended for the modelling of a fossil skull similar to *Madygenerpeton* due to the incorrect scaling in all three axes. Even though the model provides a good visual impression and seeming similarity with the original pictures, its dimensions are exceedingly erroneous.

Seven 3D models remained for further analysis, denoted according to the respective measurement devices, namely AICON, AR Crysta, AR Strato, ARTEC, CREAFORM GoScan, CREAFORM HandyScan, and EinScan Pro. In order to obtain scientifically grounded results, alignment of 3D models was performed according to the criterion of distance minimization, based on a sufficient number of repetitions. First, the common points were set in the manual mode for each couple of models, using 5 points for each analysis. Mathematically, it is enough to choose 3 common points to align two models in 3D space. To increase the accuracy, however, 5 points were chosen and minimization of the mean distance between them was performed for each couple. Second, alignment was done in the automatic mode for all models together on the entire surface. Here, 2000 randomly chosen points, uniformly distributed on the surface, were selected by the program. Alignment was performed under the condition of minimum square root distances between the 3D models, as shown in Fig. 4.

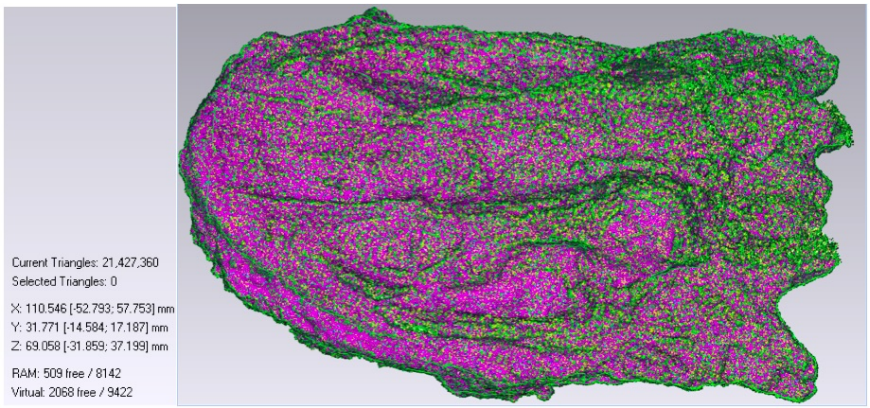

Fig. 4. Automatic alignment of the tested 3D models based on 2000 points.

3.2. Statistical analysis

After alignment, analysis of each couple of models was performed with visual assessment of the colour map of deviations. In Fig. 5, there is an examplary map, constructed for AICON and AR Crysta models. Main statistic parameters of each couple analysis are shown in Table 2. It includes maximal distances $\max\{\Delta_d\}$ and average (mean) values $\overline{\Delta_d}$ between the polygons of the tested 3D models, as well as the respective standard deviations $\sigma\{\Delta_d\}$. The average (mean) values are divided in three categories: one marked "overall" covers all distances in both outer and inner directions, the others marked "positive" and "negative" cover the distances outside and inside the reference surface, respectively.

From the practical perspective, parameters $\overline{\Delta_d}$ and $\sigma\{\Delta_d\}$ are more informative. Especially the latter one is a good measure of the difference between the surfaces represented by the tested 3D models.

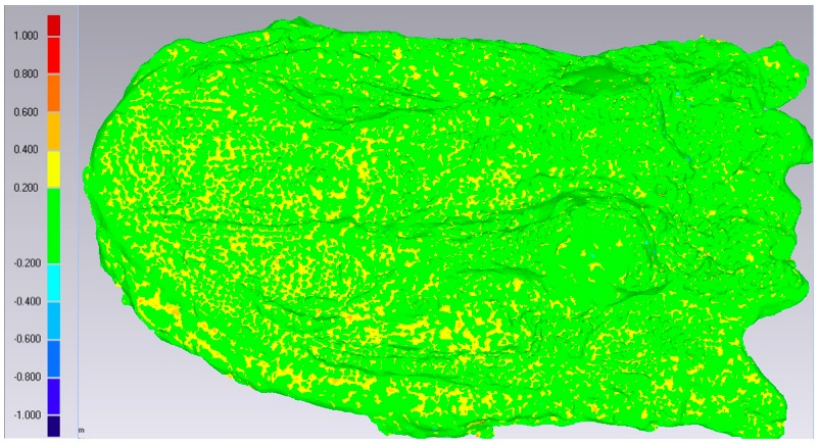

Fig. 5. Colour mapping of distances between the AR-Crysta and AICON models obtained from the Geomagic Studio CAD system.

Table 2. Statistics of the distances between the surfaces of the tested 3D models.

Reference and test model	Distance statistics [mm]			
	Average $\overline{\Delta_d}$			Standard deviation $\sigma\{\Delta_d\}$
	overall	positive	negative	
AICON – AR Crysta	0.101	0.126	–0.054	0.095
AICON – AR Strato	0.119	0.128	–0.051	0.080
AICON – ARTEC	0.036	0.056	–0.024	0.111
AICON – CREAFORM GoScan	0.074	0.115	–0.060	0.104
AICON – CREAFORM HandyScan	0.073	0.115	–0.060	0.105
AICON – EinScan Pro	0.022	0.044	–0.032	0.047
AR Crysta – AR Strato	0.009	0.077	–0.066	0.091
AR Crysta – ARTEC	–0.137	0.258	–0.301	0.709
AR Crysta – CREAFORM GoScan	–0.086	0.132	–0.323	0.705
AR Crysta – CREAFORM HandyScan	–0.083	0.128	–0.327	0.698
AR Crysta – EinScan Pro	–0,144	0,282	–0,218	0,596
AR Strato – ARTEC	–0.115	0.462	–0.279	0.803
AR Strato – CREAFORM GoScan	–0.059	0.287	–0.404	0.896
AR Strato – CREAFORM HandyScan	–0.043	0.284	–0.433	0.899
AR Strato – EinScan Pro	–0.134	0.612	–0.258	0.805
ARTEC – CREAFORM GoScan	0.044	0.105	–0.076	0.110
ARTEC – CREAFORM HandyScan	0.041	0.105	–0.076	0.111
ARTEC – EinScan Pro	–0.005	0.045	–0.052	0.061
CREAFORM GoScan – CREAFORM HandyScan	0.000	0.036	–0.035	0.042
CREAFORM GoScan – EinScan Pro	–0.062	0.055	–0.098	0.092
CREAFORM HandyScan – EinScan Pro	–0.062	0.053	–0.100	0.093

Metrol. Meas. Syst., Vol. 29 (2022), No. 1, pp. 37–51
DOI: 10.24425/mms.2022.138547

Average distances $\overline{\Delta_d}$ between every two models are presented graphically in Fig. 6 in the form of bars between the lowest and the highest values. We found it useful to distinguish between the positive direction (*i.e.* distance from the reference outer surface to the tested model) and the negative one (*i.e.* distance from the reference inner surface to the tested model). The lowest average value usually falls in the negative area, while the highest one in the positive.

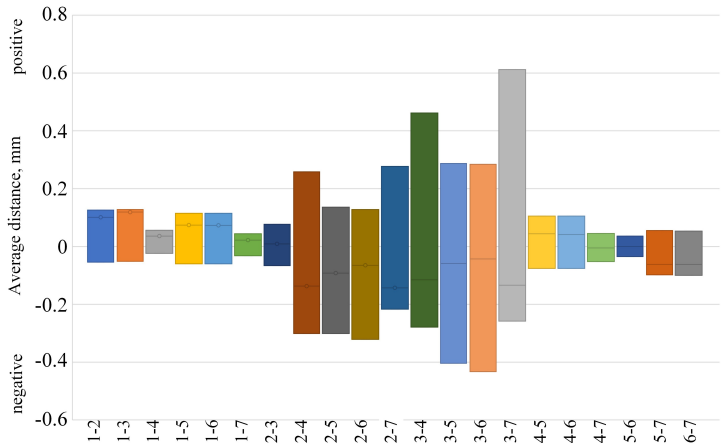

Fig. 6. Graphical representation of average distances between the tested surface models: 1. AICON, 2. AR Crysta, 3. AR Strato, 4. ARTEC, 5. CREAFORM GoScan, 6. CREAFORM HandyScan, 7. EinScan Pro.

Due to unavailability of a reference model, the assumption was made that the models with the smallest differences represent the original surface more accurately. The couples created by AR Crysta and AR Strato with ARTEC, CREAFORM GoScan, HandyScan, and EinScan Pro can be clearly distinguished from the results seen in Fig. 6. Here, the distances in both directions are larger than elsewhere. In order to check this observation, an additional graph was plotted, shown in Fig. 7. This graph reflects two main statistical parameters, namely, average (mean) and standard

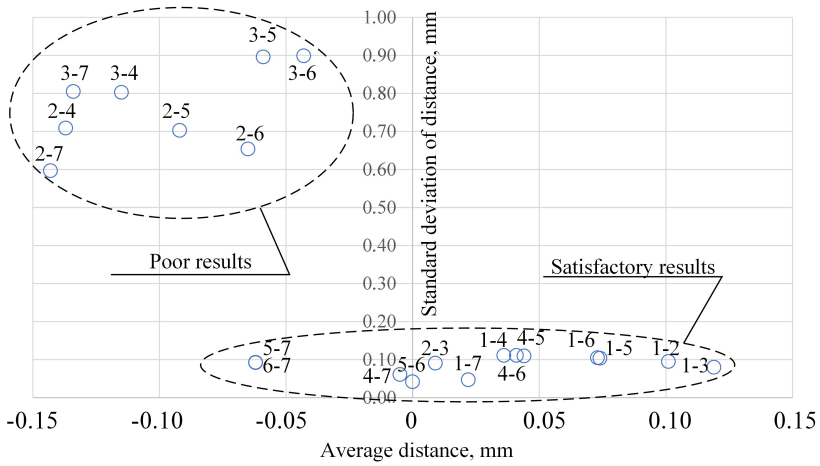

Fig. 7. Comparative analysis of standard deviations versus average distances for the couples of 3D models: 1. AICON, 2. AR Crysta, 3. AR Strato, 4. ARTEC, 5. CREAFORM GoScan, 6. CREAFORM HandyScan, 7. EinScan Pro.

deviation of the analysed distances Δd between all the models put in couples. Interestingly, the obtained results formed two distinguishable groups, with substantially different standard deviations $\sigma\{\Delta_d\}$ between the tested 3D models. One of them can be considered satisfactory, while the other provided too poor results.

Standard deviation $\sigma\{\Delta_d\}$ well reflected the essence of the geometry differences between the tested 3D models, so that the couples with the largest differences fell into the first group of standard deviation $\sigma\{\Delta_d\} > 0.5$. An important observation can be made that no couple containing the AICON model is found in this group, which can substantiate conclusion that this model reflects the measured surface best. The devices AR Crysta and AR Strato generated models of quite similar geometry, but both of them can be found in the first group.

It should be noted, however, that the digital models obtained from both Mitutoyo devices can differ from others because of the measurement strategy. Namely, the cloud of points was collected from the upper side of the skull only, while with other devices, the scanning procedure was performed both from sides and from the top, and the obtained points were connected to one 3D model. However, a series of additional experiments should be done to assess the accuracy of the possible closed models that include upper and lower surfaces connected together, obtained from AR Crysta and AR Strato. At the present stage of research, without analysing of individual sources of inaccuracy [40], we can only state that these models found themselves in the group with poor results. Moreover, they are also present in the second group in couples of the largest average distances $\overline{\Delta_d} > 0.1$ mm from the AICON model. Similar geometry was obtained by the following couples: ARTEC – EinScan Pro; ARTEC – CREAFORM GoScan; ARTEC – CREAFORM HandyScan; CREAFORM GoScan – CREAFORM HandyScan.

3.3. Rating of the models

From the statistical analysis of the differences in each couple of models, it is possible to derive a rating of those providing similar geometry in a larger number of couples. Namely, using a minimal distance $\overline{\Delta_d}$ and minimal standard deviation criteria $\sigma\{\Delta_d\}$, it can be assumed that the device with the largest number of couples of smallest differences is reflecting features and dimensions of the *Madygenerpeton* skull with the highest accuracy, while one constituting a large number of couples with large differences is less accurate. For example, taking the AICON model denoted (1) in Fig. 7, we could find 6 other models in couples with it providing "satisfactory results", which we can consider as "close models". On the other hand, the ARTEC model denoted (4) can be found 4 times in the "satisfactory results" group and 2 times in the "poor results" group. In other words, there are only 4 models close to the ARTEC results, so it should be placed lower in the rating than the AICON.

In this way, a rating list can be proposed in the following order, with the most accurate model in the first place:

1. AICON (6 close models);
2. EinScan Pro (5 close models);
3. ARTEC (4 close models);
4. CREAFORM GoScan (4 close models);
5. CREAFORM HandyScan (4 close models);
6. AR Strato (2 close models);
7. AR Crysta (2 close models).

To interpret this rating correctly, it should be kept in mind that it represents the number of closest models, not just the accuracy of the scanning method. When choosing the AICON scanner, one could expect that the obtained model will be close to 6 other models, while choosing the

Metrol. Meas. Syst., Vol. 29 (2022), No. 1, pp. 37–51
DOI: 10.24425/mms.2022.138547

AR Crysta model, only 2 others will be found close to it. This rating demonstrates that due to irregular, unknown surface characteristics of the fossil, the digital model not necessarily is the best when the most accurate device is applied.

In addition, the distances were analysed between each model and the AICON model, based on the exported data of points' coordinates, vectors and absolute values of Δd distances, from the Autodesk PowerShape program. Assuming that the AICON model reflects the fossil skull surface best, it was taken as reference. Next, analysis of differences between AICON and each other model was performed using the Box Whiskers diagram shown in Fig. 8. This diagram helps to perform an analysis of peculiarities of each 3D model in respect to the reference AICON model.

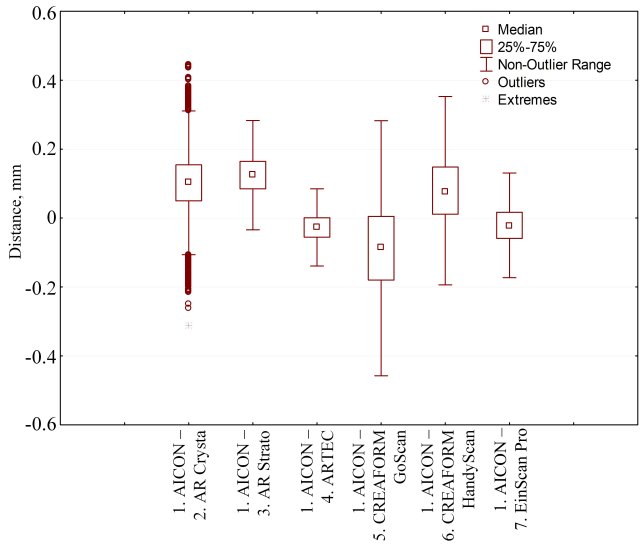

Fig. 8. Comparative analysis of differences between the AICON and every other 3D model of the *Madygenerpeton* fossil skull.

The comparative analysis of the distances Δd between the respective models was based on median, and upper and lower quartiles, as shown in Fig. 8. The results confirmed the findings obtained from the Geomagic Wrap program and the rating of the AICON model.

Taking the AICON model as reference, the best results were provided by ARTEC and EinScan Pro, with most distances Δd between respective polygons below 0.1 mm. These three devices can be recommended for digitization of a fossil skull intended for further storage in a digital repository or processing in 3D-printing technology. The largest differences occurred with the models generated by AR Crysta and CREAFORM GoScan. Here, in some areas of the tested surface, the differences are as large as 0.5 mm. Since the dimensions of some features like bony tubercles lay between 0.5 and 1.0 mm, these two devices rather should not be used in this application, at least in the way described above.

4. Conclusions

The performed comparative statistical analysis enabled the assessment of technical abilities of the scanning devices and respective 3D models for the reproduction of the complex surface and shape of the fossil skull of *Madygenerpeton*. Due to incorrect scaling in all three axes, the

model generated by photogrammetry was found unsuitable for the 3D reproduction of the skull. Further research may help to find out the conditions that would provide satisfactory results from this method.

Main statistic parameters of each couple analysis included maximal distances $\max\{\Delta_d\}$ and average values $\overline{\Delta_d}$ between the polygons of the tested 3D models, as well as the respective standard deviations $\sigma\{\Delta_d\}$. From the practical perspective, the parameters $\overline{\Delta_d}$ and especially $\sigma\{\Delta_d\}$ that represented the differences between the surfaces of the tested 3D models were found more informative. Assuming that the device with the largest number of couples of smallest differences is reflecting features and dimensions of the *Madygenerpeton* skull with the highest accuracy, a rating of the triangulated surface models could be performed.

Having a set of digital models, the proposed method made it possible to determine which one is the most accurate. In the case of analyzed devices, two groups of results were clearly distinguishable, one of which with standard deviation $\sigma\{\Delta_d\} > 0.5$ represented poor results. No couple containing the AICON model appeared in this group, which led to the conclusion that this model was the most accurate with respect to the measured surface. On the other hand, the rating list is very helpful to choose the best device among the ones that fulfil additional criteria for further similar applications, where other factors like price or object dimensions should be considered. Moreover, the results provided ground to choose the AICON model as a reference one for further investigations on the scanning strategy effect on the fidelity of the models.

The proposed approach is applicable to any other object scanned with different scanning systems with reasonably good metrological characteristics. It can be recommended for validation of scanning methods in each particular case, when no reference model is available, without necessity of detailed metrological analysis of each scanning method. In palaeontology, where objects are unique and exhibit individual geometrical features and surface textures, and thus have no reference model, the proposed approach can be applied to any particular fossil.

Acknowledgements

The research was presented and discussed at the euspen's 21st International Conference & Exhibition, Copenhagen, DK, June 2021. We thank the collection keeper Birgit Gaitzsch (Freiberg) for the permission to use the precious holotype of *Madygenerpeton pustulatum* in our research. We are indebted to several colleagues who helped with the acquisition of 3D data: Daniel Eger Passos and Sascha Schmidt (Freiberg), Maik Jähne, Henrik Alhers and Thomas Reuter (Dresden), Kristin Mahlow and Tom Cvjetkovic (Berlin), Tomasz Szymański and Robert Długoszewski (Wrocław).

The results presented in this paper were achieved in the frame of the ESF-funded young researcher group "G.O.D.S." (Geoscientific Objects Digitization Standards) at the TU Bergakademie Freiberg. This paper was supported by the Kazan Federal University Strategic Academic Leadership Program.

References

[1] Friess, M. (2012). Scratching the surface? The use of surface scanning in physical and paleoanthropology. *Journal of Anthropological Sciences*, *90*, 1–26. https:/doi.org/10.4436/jass.90004

[2] Waltenberger, L., Rebay-Salisbury, K., & Mitteroecker, P. (2021). Three-dimensional surface scanning methods in osteology: A topographical and geometric morphometric comparison. *American Journal of Physical Anthropology*, *174*, 846–858. https:/doi.org/10.1002/ajpa.24204

[3] Emam, S. M., Khatibi, S., & Khalili, K. (2014). Improving the Accuracy of Laser Scanning for 3D Model Reconstruction Using Dithering Technique. *Procedia Technology*, *12*, 353–358. https:/doi.org/10.1016/j.protcy.2013.12.498

Metrol. Meas. Syst., Vol. 29 (2022), No. 1, pp. 37–51
DOI: 10.24425/mms.2022.138547

[4] Karczewski, M. (2019). Influence of 3D scanner parameters on accuracy evaluation of vehicle element deformation. *AIP Conference Proceedings*, *2078*, 020012. https:/doi.org/10.1063/1.5092015

[5] Majchrowski, R., Wieczorowski, M., Grzelka, M., Sadowski, Ł, & Gapiński, B. (2015). Large area concrete surface topography measurements using optical 3D scanner. *Metrology and Measurement Systems*, *22*(4), 565–576. https:/doi.org/10.1515/mms-2015-0046

[6] Counts, D. B., Averett, E. W., & Garstki, K. (2016). A fragmented past: (re)constructing antiquity through 3D artefact modelling and customised structured light scanning at Athienou-*Malloura*, Cyprus. *Antiquity*, *90*, 206–218. https:/doi.org/10.15184/aqy.2015.181

[7] Grosman, L., Smikt, O., & Smilansky, U. (2008). On the application of 3-D scanning technology for the documentation and typology of lithic artefacts. *Journal of Archaeological Science*, *35*, 3101–3110. https:/doi.org/10.1016/j.jas.2008.06.011

[8] Kuzminsky, S., & Gardiner, M. (2012). Three-dimensional laser scanning: Potential uses for museum conservation and scientific research. *Journal of Archaeological Science*, *39*(8), 2744–2751. https:/doi.org/10.1016/j.jas.2012.04.020

[9] Bouby, L., Figueiral, I., Bouchette, A., Rovira, N., Ivorra, S., Lacombe, T., Pastor, T., Picq, S., Marinval, P., & Terral, J. F. (2013). Bioarchaeological insights into the process of domestication of grapevine (Vitis vinifera L.) during Roman Times in southern France. *PLoS One*, *8*(5), e63195. https:/doi.org/10.1371/journal.pone.0063195

[10] Haukaas, C., & Hoddgetts, L. M. (2016). The untapped potential of low-cost photogrammetry in community-based archaeology: A case study from Banks Island, Arctic Canada. *Journal of Community Archaeology and Heritage*, *3*, 40–56. https:/doi.org/10.1080/20518196.2015.1123884

[11] Porter, S. T., Roussel, M., & Soressi, M. (2016). A simple photogrammetry rig for the reliable creation of 3D artefact models in the field lithic examples from the early upper Paleolithic sequence of Les Cottés (France). *Advances in Archaeological Practice*, *4*, 71–86. https:/doi.org/10.7183/2326-3768.4.1.71

[12] Re, C., Robson, S., Roncella, R., & Hess, M. (2011). Metric Accuracy Evaluation of Dense Matching Algorithms in Archeological Applications. *Geoinformatics FCE CTU*, *6*, 275–282. https:/doi.org/10.14311/gi.6.34

[13] Adams, J. W., Olah, A., McCurry, M. R., & Potze, S. (2015). Surface model and tomographic archive of fossil primate and other mammal holotype and paratype specimens of the Ditsong National Museum of Natural History, Pretoria, South Africa. *PLoS One*, *10*(10), 1–14. https:/doi.org/10.1371/journal.pone.0139800

[14] Das, A. J., Murmann, D. C., Cohrn, K., & Raskar, R. (2017). A method for rapid 3D scanning and replication of large paleontological specimens. *PLoS ONE*, *12*(7), e0179264. https:/doi.org/10.1371/journal.pone.0179264

[15] Motani, R. (2005). Detailed tooth morphology in a durophagus ichthyosaur captured by 3D laser scanner. *Journal of Vertebrate Paleontology*, *25*, 462–465. https:/doi.org/10.1671/0272-4634(2005)025[0462:DTMIAD]2.0.CO;2

[16] Niven, L., Steele, T. E., Finke, H., Gernat, T., & Hublin, J. J. (2009). Virtual skeletons: Using a structured light scanner to create a 3D faunal comparative collection. *Journal of Archaeological Science*, *36*, 2018–2023. https:/doi.org/10.1016/j.jas.2009.05.021

[17] Windhager, S., Mitteroecker, P., Rupić, I., Lauc, T., Polašek, O., & Schaefer, K. (2019). Facial aging trajectories: A common shape pattern in male and female faces is disrupted after menopause. *American Journal of Physical Anthropology*, *169*(4), 678–688. https:/doi.org/10.1002/ajpa.23878

[18] Evin, A., Souter, T., Hulme-Beaman, A., Ameen, C., Allen, R., Viacava, P., Larson, G., Cucchi, T., & Dobne, K. (2016). The use of close-range photogrammetry in zooarchaeology: Creating accurate 3D models of wolf crania to study dog domestication. *Journal of Archaeological Science*, *9*, 87–93. https:/doi.org/10.1016/j.jasrep.2016.06.028

[19] Loy, A., Tamburelli, A., Carlini, R., & Slice, D. E. (2011). Craniometric variation of some Mediterranean and Atlantic populations of Stenella coeruleoalba (Mammalia, Delphinidae): A three- dimensional geometric morphometric analysis. *Marine Mammal Science*, *27*(2), E65–E78. https:/doi.org/10.1111/j.1748-7692.2010.00431.x

[20] Milne, N., Vizcaíno, S. F., & Fernicola, J. C. (2009). A 3D geometric morphometric analysis of digging ability in the extant and fossil cingulate humerus. *Journal of Zoology*, *278*(1), 48–56. https:/doi.org/10.1111/j.1469-7998.2008.00548.x

[21] Munoz-Munoz, F., Quinto-Sanchez, M., & Gonzales-Jose, R. (2016). Photogrammetry: A useful tool for three dimensional morphometric analysis of small mammals. *Journal of Zoological Systematics and Evolutionary Research*, *54*(4), 318–325. https:/doi.org/10.1111/jzs.12137

[22] Owen, J., Dobney, K., Evin, A., Cucchi, T., Larson, G., & Vidarsdottir, U. S. (2014). The zooarchaeological application of quantifying cranial shape differences in wild boar and domestic pigs (Sus scrofa) using 3D geometric morphometrics. *Journal of Archaeological Science*, *43*, 159–167. https:/doi.org/10.1016/j.jas.2013.12.010

[23] Haleem, A., & Javaid, M. (2018). 3D scanning applications in medical field: A literature-based review. *Clinical Epidemiology and Global Health*, *7*(2), 199–210. https:/doi.org/10.1016/j.cegh.2018.05.006

[24] Elkhuizen, W. S., Callewaert, T. W. J., Leonhardt, E., Vandivere, A., Song, Y., Pont, S. C., Geraedts J. M. P., & Dik, J. (2019). Comparison of three 3D scanning techniques for paintings, as applied to Vermeer's 'Girl with a Pearl Earring'. *Heritage Science*, *7*, 89. https:/doi.org/10.1186/s40494-019-0331-5

[25] Sousa, E, Vieira, L, Costa, D. M. S., Costa D. C., Parafita, R., & Loja, M. A. R. (2017). Comparison between 3D laser scanning and computed tomography on the modelling of head surface. *Proceedings of the 3rd International Conference on Numerical and Symbolic Computation – SYMCOMP 2017*, Guimarães, Portugal, 119 – 128.

[26] Pawlus, P., Reizer, R., & Wieczorowski, M. (2018). Comparison of results of surface texture measurement obtained with stylus methods and optical methods. *Metrology and Measurement Systems*, *25*(3), 589–602. https:/doi.org/10.24425/123894

[27] Hawryluk, M., Ziemba, J., & Dworzak, Ł. (2017). Development of a method for tool wear analysis using 3D scanning. *Metrology and Measurement Systems*, *24*(4), 739–757. https:/doi.org/10.1515/mms-2017-0054

[28] Rudolph, H., Luthardt, R. G., & Walter, M. H. (2007). Computer-aided analysis of the influence of digitizing and surfacing on the accuracy in dental CAD/CAM technology. *Computers in Biology and Medicine*, *37*(5), 579–587. https:/doi.org/10.1016/j.compbiomed.2006.05.006

[29] Nedelcu, R. G., & Persson, A. S. K. (2014). Scanning accuracy and precision in 4 intraoral scanners: An in vitro comparison based on 3-dimensional analysis. *Journal of Prosthetic Dentistry*, *112*(6), 1461–1471. https:/doi.org/10.1016/j.prosdent.2014.05.027

[30] Smith, E. J., Anstey, J. A., Venne, G., & Ellis, R. E. (2013). Using additive manufacturing in accuracy evaluation of reconstructions from computed tomography. *Proceedings of the Institution of Mechanical Engineers, Part H: Journal of Engineering in Medicine*, *227*(5), 551–559. https:/doi.org/10.1177/0954411912474612

[31] Zhao, Y., Xiong, Y., & Wang, Y. (2017). Three-Dimensional Accuracy of Facial Scan for Facial Deformities in Clinics: A New Evaluation Method for Facial Scanner Accuracy. *PLOS ONE*, *12*(1), e0169402. https:/doi.org/10.1371/journal.pone.0169402

[32] Kim, Y. H., Han, S.-S., Choi, Y. J., & Woo, C.-W. (2020). Linear Accuracy of Full-Arch Digital Models Using Four Different Scanning Methods: An In Vitro Study Using a Coordinate Measuring Machine. *Applied Sciences*, *10*(8), 2741. https:/doi.org/10.3390/app10082741

Metrol. Meas. Syst., Vol. 29 (2022), No. 1, pp. 37–51
DOI: 10.24425/mms.2022.138547

[33] Aly, P. S., & Mohsen, Ch. A. (2020). Evaluation of the accuracy of digital models obtained from intraoral scanners with different CAD/CAM scanning technologies – An in vitro study. *Alexandria Dental Journal*, *45*(3), 94–98. https:/doi.org/10.21608/ADJALEXU.2020.118538

[34] Cunningham, J. A., Rahman, I. A., Lautenschlager, S., Rayfield, E. J., & Donoghue, Ph. C. J. (2014). A virtual world of paleontology. *Trends in Ecology & Evolution*, *29*(6), 347–357. https:/doi.org/10.1016/j.tree.2014.04.004

[35] Díez Díaz, V., Mallison, H., Asbach, P., Schwarz, D. & Blanco, A. (2021). Comparing surface digitization techniques in palaeontology using visual perceptual metrics and distance computations between 3D meshes. *Palaeontology*, *64*(2), 179-202. https:/doi.org/10.1111/pala.12518

[36] Kogan, I., Rucki, M., Jähne, M., Eger Passos, D., Cvjetkovic, T. & Schmidt, S. (2020). One Head, Many Approaches – Comparing 3D Models of a Fossil Skull. In Luhmann, Th., & Schumacher, Ch. (Eds.). *Photogrammetrie – Laserscanning – Optische 3D-Messtechnik: Beiträge der Oldenburger 3D-Tage 2020* (pp. 22–31). Wichmann Verlag, Berlin.

[37] Garashchenko, Y., Kogan, I., & Rucki, M. (2021). Analysis of 3D triangulated models of *Madygenerpeton pustulatum* fossil skull. *Proceedings of the euspen's 21st International Conference & Exhibition*, Denmark, 89–90.

[38] Schoch, R. R., Voigt, S., & Buchwitz, M. (2010) A chroniosuchid from the Triassic of Kyrgyzstan and analysis of chroniosuchian relationships. *Zoological Journal of the Linnean Society*, *160*, 515–530. https:/doi.org/10.1111/j.1096-3642.2009.00613.x

[39] Mallison, H. & Wings, O. (2014). Photogrammetry in paleontology – a practical guide. Journal of Paleontological Techniques, 12, 1–31.

[40] Wójcik, A., Niemczewska-Wójcik, M., & Sładek, J. (2017). Assessment of Free-Form Surfaces' Reconstruction Accuracy. *Metrology and Measurement Systems*, *24*(2), 303–312. https:/doi.org/10.1515/mms-2017-0035

Yaroslav Garashchenko obtained his Ph.D. degree in mechanical engineering from the National Technical University "Kharkiv Polytechnic Institute", Kharkiv, Ukraine, in 2004. He is currently Associated Professor at the Department of Integrated Technologies of Mechanical Engineering of the National Technical University "Kharkiv Polytechnic Institute" in Kharkiv, Ukraine. His research activity focuses primarily on reverse engineering and additive manufacturing process planning. He has authored or coauthored 3 books, over 60 journal and conference publications.

Ilja Kogan teaches vertebrate palaeontology in Freiberg, Germany where he obtained his M.Sc. diploma in geology in 2008 and the Ph.D. degree in palaeontology in 2016. He is also a research fellow at the Federal University of Kazan, Russia. His interests comprise the evolution and diversity of fish during the Late Palaeozoic and Mesozoic and in the application of digital methods to fossils, and currently leads a group of young researchers developing digitization standards for geoscientific objects. He has authored or co-authored some 30 publications and over 65 conference papers.

Miroslaw Rucki obtained M.Sc. and Ph.D. degrees in mechanical engineering from the Poznań University of Technology, Poznań, Poland, in 1993 and 1997, respectively. He is currently Associate Professor with the Kazimierz Pulaski University of Technology and Humanities in Radom, Poland. His research activity focuses primarily on measurement of geometrical values, form deviations and metrological analysis of various measurement systems. He has authored or coauthored 2 books, a dozen of book chapters, over 100 journal publications and 80 conference papers.